σ = 0.5and 0.3 with peak values of 2.5 K per day, and cooling in the top layer (σ = 0.1) at half this rate. This cooling represents anomalous radiative cooling at cloud top as measured by the OLR anomaly. The upper tropospheric heating in a 400-mb layer follows D. L. Hartmann, H. H. Hendon, R. A. Houze [*J. Atmos. Sci.* **41**, 113 (1984)]. At 5°N the sign of the vertical profile of forcing is reversed.
20. R. Mureau, J. D. Opsteegh, J. D. Winston, *Mon. Weather Rev.* **115**, 856 (1987).
21. Other preliminary experiments support the robustness of our results. When the climatological waves are retained, the structure of the response is rather insensitive to the exact longitude of the heating. Point sources at all locations at 15°N between 100° and 150°W, but not elsewhere, produce essentially the same midlatitude pattern, although with varying amplitude. Changes in the vertical heating profile in the model also alter the amplitude but not the pattern of the response.
22. K. Kurihara and T. Tsuyuki, *J. Meteorol. Soc. Jpn.* **65**, 237 (1987); T. Nitta, *ibid.*, p. 373.
23. W. D. Sellers, *Physical Climatology* (Univ. of Chicago Press, Chicago, 1965); J. Shukla and Y. Mintz, *Science* **215**, 1498 (1982); T.-C. Yeh, R. T. Wetherald, S. Manabe, *Mon. Weather Rev.* **112**, 474 (1984).
24. P. D. Sardeshmukh and B. J. Hoskins, *J. Atmos. Sci.* **45**, 1228 (1988).
25. G. Branstator, *J. Atmos. Sci.* **40**, 1689 (1983), P. A. Webster and J. Holton, *ibid.* **39**, 722 (1982).
26. A. Simmons, J. M. Wallace, G. Branstator, *J. Atmos. Sci.* **40**, 1363 (1983).
27. S. E. Zebiak and M. A. Cane, *Mon. Weather Rev.* **115**, 2262 (1987).
28. The National Center for Atmospheric Research is sponsored by the National Science Foundation.

Laser Femtochemistry

AHMED H. ZEWAIL

Femtochemistry is concerned with the very act of the molecular motion that brings about chemistry, chemical bond breaking, or bond formation on the femtosecond (10^{-15} second) time scale. With lasers it is now possible to record snapshots of chemical reactions with sub-angstrom resolution. This strobing of the transition-state region between reagents and products provides real time observations that are fundamental to understanding the dynamics of the chemical bond.

THE MOLECULAR EVENTS THAT BRING ABOUT CHEMISTRY, chemical bond breaking or bond formation, occur with awesome rapidity, often in less than 10^{-12} s. One of the fundamental problems in chemistry is to understand how these events, which occur in the region of the transition state between reagents and products, determine the entire course of the reaction, including the fate of the products. In the past the actual dynamics of this region could not be time-resolved, but chemists devised methodologies for describing reactivity. Different approaches (for example, thermodynamics, kinetics, and synthesis) have been used to systematize a large body of experimental data and obtain the energetics (ΔG, ΔH, and so forth), the rates [$k(T)$], and the mechanisms of the reactions, thus establishing the macroscopic picture.

Understanding the detailed dynamics of reactions on the molecular level required new microscopic methods (*1–3*), which were introduced some 30 years ago. Major advances have come from the application of molecular beam, chemiluminescence, and laser techniques (*4*). In the simplest molecular beam experiments, a beam of reagent molecules is directed towards co-reagent molecules (in the form of a target gas or another beam), and the reactive scattering that leads to product molecules is observed. The relative kinetic energy of the reagents can be changed by varying the velocity of one of the reagent molecules with respect to the other reagent involved in the "single collision." For laser–molecular beam experiments, a laser can be used to excite one of the reagent molecules and thus influence the reaction probability, or the laser can initiate a unimolecular process by depositing energy in a molecule. In this so-called "half-collision" unimolecular process, the fragmentation of the excited molecule, which can be represented as ABC into A and BC, is the dynamical process of interest.

The ingeniousness of this approach is in using the postcollision (or half-collision) attributes of the products (angular distributions, population and energy distributions, alignment, and so forth) to infer the dynamics of the reactive collision (or half-collision). During the last three decades many reactions have been studied and these methods, with the help of theory, have become the main source of information for deducing the nature of the potential energy surface (PES) of the reaction (*4*).

To directly observe the transition-state region between reagents and products, which is the fundamental feature of reaction dynamics, different methodology is needed. As mentioned above, these states are ultrashort-lived and experiments on a longer time scale provide data that are effectively time-integrated over the course of the collision or half-collision. Smith (*5*), in comparing different experimental approaches, noted that a great deal is known about the "before" and "after" stages of the reaction, but that it is difficult to observe the "during" phase. The problem is perhaps illustrated best by the quotation of Zare and Bernstein (*6*), which describes the choreography of these processes: "The study of chemical reaction kinetics can be likened to the task of making a motion picture of a reaction. The trouble thus far with achieving this goal seems to be the problem of too many would-be actors who strut upon the stage without proper cue and mumble their lines too rapidly to be understood—for chemical reactions occur with the ease of striking a match and at a speed so fast (on a subpicosecond time scale for the making of new bonds and breaking of old ones) as to be a severe challenge to the moviemaker who would like to record individual frames."

In recent years, great progress has been made by several groups (*7–13*) using absorption, emission, scattering, and ion spectroscopy to probe the relevant transition region. Without direct time resolution, they used these clever methods, reviewed recently by Polanyi (*7*), Kinsey (*8*), and Brooks and Curl (*9*), to obtain information on the dynamics in the transition-state region of some elementary reactions. Examples include the dissociation of methyl iodide (*8*)

The author is a professor of chemistry at the Arthur Amos Noyes Laboratory of Chemical Physics, California Institute of Technology, Pasadena, CA 91125.

and of sodium iodide (7). The experiments are on a longer time scale than the lifetime of transition states, but in the spectra the time evolution of these states is reflected, although it is unresolved. Even picosecond real-time studies of reactions (*14*) are inadequate for direct observations in the transition-state region.

Real-time femtochemistry, that is, chemistry on the femtosecond time scale, can be defined (*15*) as the field of chemical dynamics concerned with the very act of breaking or making a chemical bond. On this time scale the molecular dynamics are "frozen out," and thus one should be able to observe the complete evolution of the chemical event, starting from time zero, passing through transition states, and ultimately forming products. As shown below, this time scale is perhaps the ultimate one as far as chemistry is concerned, but future studies need not necessarily terminate with this time resolution. Ultimately such experiments are limited by the uncertainty principle.

Ultrafast laser techniques are the essential part of femtochemistry, and permit the initiation and recording of snapshots of chemical reactions with femtosecond time resolution (*16–22*). With these pulses, sub-angstrom motion can be resolved since the recoil velocity of fragments is typically 1 km s^{-1}. It is also possible to work with molecules expanded in supersonic beams or jets; the expansion extensively cools the reactant molecules, which simplifies their internal energy distribution and makes it easier to perform "state-to-state" experiments (for example, between particular vibrational states) under collisionless condition. However, since collisions are on a much longer time scale than femtoseconds, experiments can also be carried out in bulk gases.

The objective of this article is to describe the concepts involved and to highlight recent developments in real-time laser femtochemistry. Reaction dynamics in collisional environments, including condensed phases, is beyond the scope of this article; however, the importance of the femtosecond time scale in probing primary chemical processes in condensed media and in biological systems will become clear.

The techniques and some examples of elementary reactions that have recently been studied are focused on below.

Femtochemistry and the Time Scale of Reactions

Of particular interest are the dynamics of elementary reactions, such as

$$ABC^* \rightarrow [A \cdots BC]^{\ddagger *} \rightarrow A + BC \text{ (unimolecular)}$$

$$A + BC \rightarrow [ABC]^{\ddagger} \rightarrow AB + C \text{ (bimolecular)}$$

In these reactions, a single chemical bond is broken or formed, and one can examine the process fundamentally. However, the bond is broken (or formed) so rapidly that direct measurements have not been previously possible. An estimate of the time for bond breaking can be made as follows: The terminal velocities of separation of the fragments A and BC are typically ~0.01 Å fs^{-1}. If the bond is considered to be broken when the fragments are a few times their equilibrium bond length apart (typically, several angstroms), then the time required to break the bond must be of the order of a few hundred femtoseconds. During this time period, the system passes through transition states.

Strictly defined, the transition state of a reaction is a "configuration of no return" such that once the system has passed this critical spatial configuration it necessarily proceeds to form products. This state is frequently associated with a barrier along the reaction path, such as a saddle point. As other authors have done (*7–12*), the term transition states is used here to refer not only to this one particular state, but rather to all of the intermediate states along the reaction

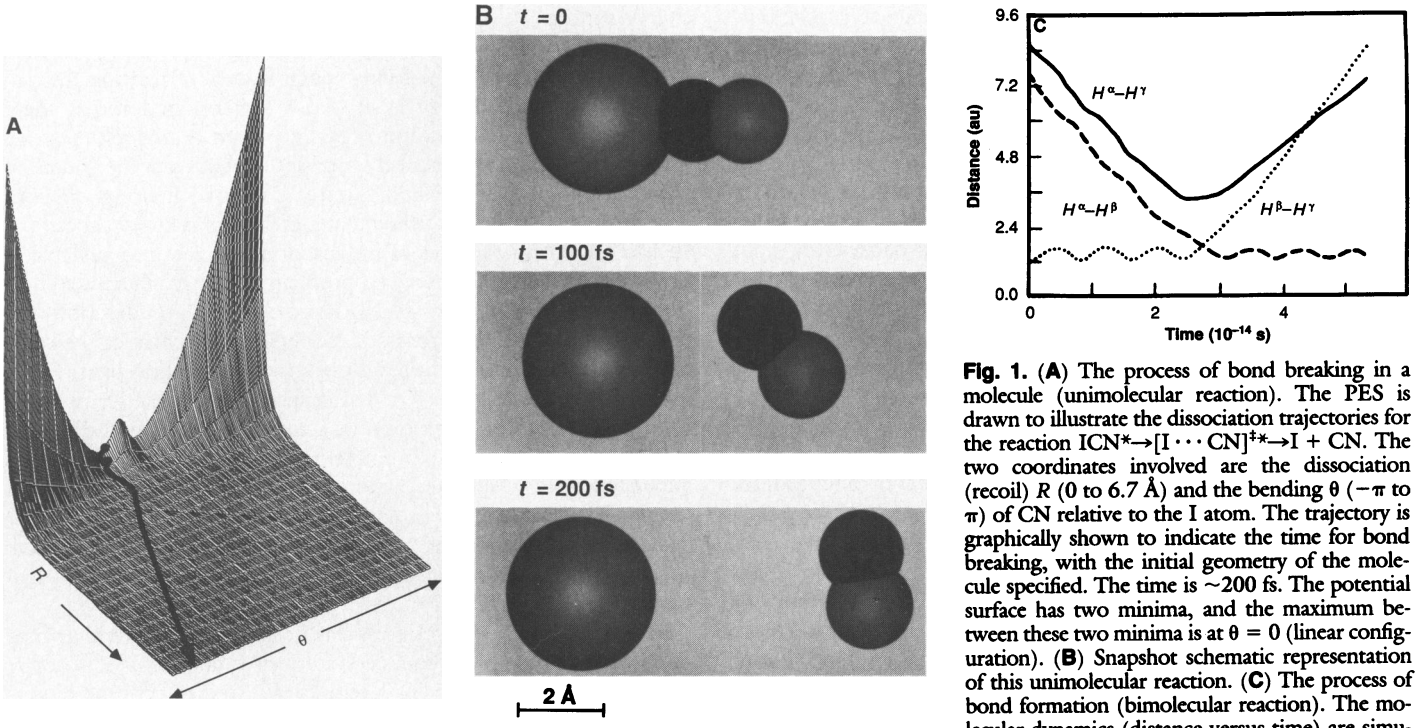

Fig. 1. (**A**) The process of bond breaking in a molecule (unimolecular reaction). The PES is drawn to illustrate the dissociation trajectories for the reaction ICN*→[I···CN]‡*→I + CN. The two coordinates involved are the dissociation (recoil) R (0 to 6.7 Å) and the bending θ ($-\pi$ to π) of CN relative to the I atom. The trajectory is graphically shown to indicate the time for bond breaking, with the initial geometry of the molecule specified. The time is ~200 fs. The potential surface has two minima, and the maximum between these two minima is at $\theta = 0$ (linear configuration). (**B**) Snapshot schematic representation of this unimolecular reaction. (**C**) The process of bond formation (bimolecular reaction). The molecular dynamics (distance versus time) are simulated for the reaction $H^{\alpha} + H^{\beta} - H^{\gamma}$, with a time resolution of femtoseconds. The H–H molecule vibrates on this time scale, and when the H atom approaches the H–H molecule, the three hydrogens of the H_3 species "stick" together for about 10 fs. Products are then formed. The femtochemistry of this reaction occurs in 10 fs, and this time, relative to the vibrational and rotational periods of H_3, determines the fate of products [see (*25*)].

path that are sufficiently removed from the reagent and product states so as to be experimentally distinguishable from them. It is precisely this region that defines the dynamics during the half-collision (for dissociation reactions) or full-collision (for bimolecular reactions).

Theoretical femtochemistry dates from the 1930s, following the introduction of the concept of the transition state by Evans, Polanyi, and Eyring (*23*). In 1936, Hirschfelder, Eyring, and Topley (*24*) calculated point-by-point the classical-mechanical trajectory of a free hydrogen atom approaching an H_2 molecule to form an "activated complex" or transition state in the reaction H + H_2. In this and all subsequent classical trajectory simulations (see Fig. 1) of elementary chemical reactions, pioneered by Karplus, Bunker, Polanyi, and others (*25, 26*), it became evident that femtosecond time resolution is required to view the "moment of the collision," even in reactions like H + H_2 (at the time, no ultrashort time pulses could be generated to provide such temporal resolution; recall that flash photolysis was first begun in 1949 with a time resolution of only milliseconds).

These calculations formed the theoretical ideas about transition-state chemistry which can now be realized experimentally. The tool for this research (*16–22*) is femtosecond transition-state spectroscopy (FTS) of reactions, which is described below. The combination of ultrashort pulsed-laser interferometric and molecular beam techniques has made this possible [see (*13, 14, 16–21*)]. Optical pulses as short as 6 fs can be generated, following the pioneering design of dye lasers by Shank and colleagues (*27*) and used in FTS.

Spectra of the Transition-State Region

Transient species, which are intermediate between reagents and products, are expected to have different spectra from those of the stable products or reagents. For these intermediate species, the transition energies and spectral linewidths are shifted and broadened because of perturbations caused by the close proximity of product fragments (*28*).

Polanyi's group (*7*) has used the emission of fragments in the course of a reaction to record the broad wing spectra (to the blue or the red of the free fragment transition) characteristic of the transition region. Two reactions have been studied:

$$NaI^* \rightarrow NaI^{\ddagger *} \rightarrow Na^* + I$$

$$F + Na_2 \rightarrow [NaNaF]^{\ddagger *} \rightarrow Na^* + NaF$$

As discussed below, for the first of these reactions, femtochemistry observations have been made recently by Rose *et al.* (*18*) and Rosker *et al.* (*19*). For the bimolecular reaction, no lasers need be used since the sodium product Na* emits light. The transition state species, for example, $[NaNaF]^{\ddagger *}$, has a lifetime of 10^{-12} s or less, whereas the lifetime of free fragment Na* is about 10^{-8} s. Thus the yield of light emission from the transition state is $\sim 10^{-4}$ of that from the Na product. The wing emission reported extends over several hundred angstroms from the Na *D* line, and thus the relative intensity of the two emissions at a given wavelength is less than the anticipated 10^{-4} by still another factor of 100 or so. This effect is due to the large spectral breadth of the extended wings. Stimulated by this approach, Polanyi's group has examined potential energy models for these and other reactions with particular focus on transition-state spectroscopy. More recently, they studied the reaction of hot hydrogen atoms with deuterium molecules, and evidence for a transient species $HD_2^{\ddagger}$ was presented (*29*). Such studies are valuable to the important reactions of the H_3 family.

Kinsey's group (*8*) has advanced a (near-resonant) Raman scattering method and showed that one could use the measurements to characterize the dynamics along the reaction coordinate of molecules in the process of dissociation. The concept involved is easily visualized with the help of wave packet theory, as developed by Heller (*30*). Basically, if a laser prepares a packet of excited molecules on a repulsive PES, this packet moves in time to greater internuclear distances and spreads out. Classically, this effect is equivalent to a molecule decreasing its potential energy and converting it to translational energy (dissociation). The Raman-shifted spectral wavelengths depend on the ground-state characteristics, but the intensities of these transitions reflect the evolution of the wave packet on the upper surface. From such specta, Kinsey and coworkers deduced the nature of the excited-state surface.

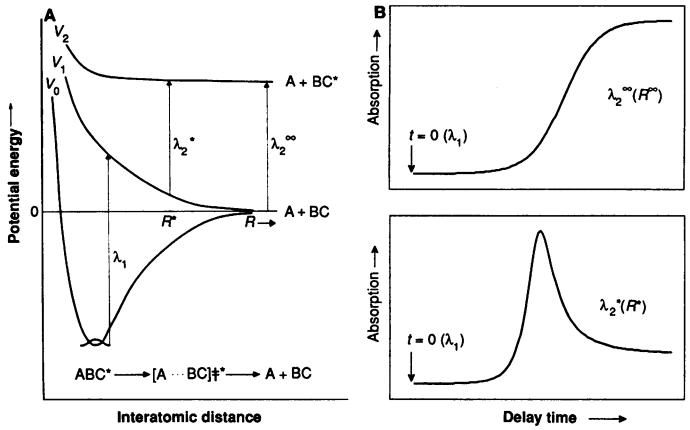

Fig. 2. The concept of observing the transition region of a reaction and the idea of an FTS experiment. (**A**) The potential energy curves are for a bound molecule (V_0), and for the first and second dissociative curves, V_1 and V_2. The repulsion between fragments on V_1 and V_2 leads to bond breaking. The pump femtosecond pulse (λ_1) takes the molecule from V_0 to V_1. As the fragments recoil, the pulse at λ_2^* (or $\lambda_2\infty$) probes the transition region (or the free fragments). (**B**) The expected femtosecond transients, signal versus delay time between pump and probe pulses, at λ_2^* and $\lambda_2\infty$.

Brooks and Curl (*9*) have invoked an absorption method to study the transient intermediate in some bimolecular reactions. As was also the case in the two previous examples, the lasers used had much longer pulse durations [nanoseconds or continuous-wave (CW) mode] than the collision complex, which lasts on the order of picoseconds. Thus the number of molecules probed, and hence the light absorption during its lifetime, is extremely small. For the reaction studied,

$$K + NaCl \longrightarrow [KClNa]^* \rightarrow KCl + Na$$

the laser was tuned to wavelengths where neither reagents (K + NaCl) nor products (KCl + Na) absorb, so the signal is attributed to the transient complex. The sensitivity issue is important in these experiments, as Brooks has recently pointed out in a review article (*9*): "The problem facing the experimentalist [when the yield of emission or absorption is very small] is to design a system where the effect of photon absorption [or emission] during collision can be observed and separated from other more 'mundane' effects."

More recently, Neumark (*10*) and Valentini (*12*) have reported on the use of photodetachment and coherent anti-Stokes Raman scattering (CARS) techniques to deduce characteristics of the transition region of two classes of reactions, namely Cl + HCl and H + H_2. All of these studies of the transition-state region represent great progress in the field and have provided new experimental insight beyond those obtained from the earlier conventional methods. Implicit in these measurements are the femtosecond dynamics, but they are time unresolved.

Femtochemistry in Real Time

Because transition states exist only for picoseconds or less, observing them directly in real time requires femtosecond time resolution. In steady-state detection, the number of molecules in the transition state is less than that of free fragments by four to six orders of magnitude, as discussed above. Accordingly, if ultrashort pulses are used, the sensitivity of the detection is enhanced by a factor of 10^4 to 10^6 when compared with steady-state experiments. Nearly all of the molecules traversing the transition states can be detected, which is a key feature of real-time femtochemistry. The difficulty, however, comes in generating reliable and tunable pulses and in developing the techniques for monitoring reactions on the femtosecond time scale. The main technique described here is FTS, which is a pump-probe method that allows snapshots of reactions to be obtained while the fragments are separating or encountering each other.

The concept of FTS. The PESs for the molecule being studied (depicted as ABC) are initially assumed to be particularly simple, as shown in Fig. 2. Such PESs are in fact typical for many real molecules undergoing direct bond breaking and have been invoked to describe theories of photodissociation. Furthermore it is also assumed that the only relevant configurational parameter is R, the internuclear separation of the fragments in the center-of-mass frame. That is, the PESs are taken to have no angular dependence, as would be the case for a quasi-diatomic molecule. Initially, the molecule is in its lowest PES, V_0. This surface, which represents the bound state of the molecule, has a well-defined minimum that occurs at an equilibrium internuclear separation R_e.

The FTS experiment begins with an ultrafast optical pulse, with wavelength $\lambda_1 \equiv \lambda_{pump}$, that initiates the reaction. As a rule, all times are taken to be relative to the temporal midpoint of this pump pulse (the "zero-of-time"). The initial internuclear separation R_0 is defined as the distance between the fragments at $t = 0$. In general, $R_0 \neq R_e$, but the excursion of the molecule within the potential well typically is not great.

Absorption of a photon involves the "instantaneous," vertical transition of the molecule from a lower lying PES (in this case, V_0) to an excited PES (V_1). The absorption of the photon is appreciable only if at R_0 the difference in the potentials of the two surfaces is nearly equal to the energy of the pump photon, that is, $V_1(R_0) - V_0(R_0) \approx hc/\lambda_1$; where h is Planck's constant and c is the speed of light. The excited molecules prepared by the pump pulse at $t = 0$ evolve for $t > 0$. The subsequent time evolution of the system wave packet is entirely determined by the details of the excited-state PES. Classically the molecules fall along V_1, with $R \rightarrow \infty$ as $t \rightarrow \infty$.

After the molecule evolves for some time delay, $t = \tau$, it is irradiated by the second femtosecond (probe) pulse, with wavelength $\lambda_2 \equiv \lambda_{probe}$. The probe pulse can only be absorbed if the transition-state configuration of the system at time τ is appropriate for a vertical transition from V_1 to a highly excited PES, V_2. Those configurations that allow for absorption of the probe photon are called the optically coupled region of the PES by the probe. This region depends on: (i) the difference between the appropriate PESs as a function of the internuclear separation, $V_2(R) - V_1(R)$, and (ii) the frequency and spectral width of the probe pulse.

The FTS signal is some measure of the absorption by the fragment of the probe pulse as a function of the time delay between pump and probe, τ, and could be recorded, for instance, by measuring the change in the transmission of the probe. Since the absorption experiment would not be background-free, far better sensitivity can be obtained through, for instance, the detection of the laser-induced fluorescence (LIF), or the multiphoton ionization (MPI) generated by the probe. Typically the FTS signal is measured when λ_2 is tuned to the absorption wavelength of the free fragment, $\lambda_2\infty$ (where ∞ denotes that $R \rightarrow \infty$) and at a number of wavelengths absorbed by the transition states λ_2* (where * denotes the transition-state region of R). Then a "surface" of measurements $A(t; \lambda_{2(a)}^*, \lambda_{2(b)}^*, \ldots, \lambda_2\infty)$ is constructed. This surface is related to the dynamics and to the PES of the reaction.

Clocking of reactions. In the simplest FTS experiment (clocking), the probe is centered at an absorption of one of the free fragments. In this case, the absorption of the probe initially is negligible, and becomes substantial only when the fragments achieve large internuclear distance and thus are (essentially) non-interacting. The delay at which the probe absorption "turns on," $\tau_{1/2}$, is thus a direct measurement of the time required for complete (or nearly complete) internuclear separation. In other words, FTS provides a "clock" of the time required to break the bond, and thus is a fundamental measurement.

The experiment can be pictured simply as a measure of the femtosecond "time-of-flight" on the excited-state PES from the initially excited configuration at R_0 to the free-fragment configuration, where the probe opens a "window" on the PES. If the

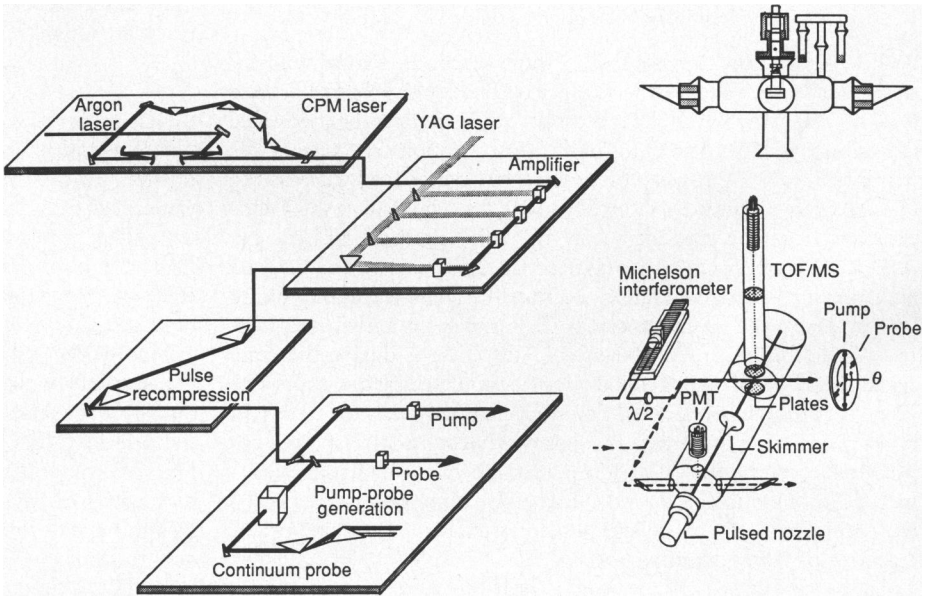

Fig. 3. The femtochemistry apparatus. The ultrafast pulses are generated in the CPM laser and are amplified in the pulsed dye amplifier. After the amplifier, the pulses are broadened temporally, which is compensated for with recompression methods (prisms arrangement). The pump and probe pulses are generated through a variety of frequency conversion sehemes and are directed into the sample chamber. The chamber is either a gas cell (upper right) or a molecular beam (lower right); TOF/MS, time-of-flight mass spectrometer; PMT, photomultiplier tube [see (*21*)].

experiment is performed for various probe spectral widths, then additional information on the asymptotic shape of the PES can be obtained. Additionally, the clocking experiment offers significant practical advantages that have been discussed by Rosker *et al.* (*21*) and Dantus *et al.* (*22*).

Detuning and detection of transition states. FTS experiments can also be performed by tuning λ_2 away from the transition of the free fragment. The final products thus do not absorb the probe wavelength, but instead the transition states of the reaction may do so. The FTS transient would be expected to build up as the molecules enter the optically coupled region, and then subsequently decay as the molecules move on to final products. The FTS transients for various values of λ_2* yield information on the shape of the PESs.

The FTS results obtained in the off-resonant experiment can be compared with those from the on-resonant (clocking) experiment. Since every molecule that enters any given transition state eventually achieves the final state, the on-resonant FTS transient should be related to an integral of an off-resonant transient. The constant of proportionality here has interesting physical significance, since it is related to both the size of the optically coupled region and the fragment velocity through it, as well as to possible oscillator strength differences. Measurements of probe absorption are dependent on the relative changes of the potentials V_1 and V_2 with time.

In cases where the dynamics on V_1 is desired, the probe wavelength can be fixed while varying the pump wavelength. In this way the recoil energy on V_1 is changed. In the center-of-mass frame:

$$E = \tfrac{1}{2}\,\mu_{A,BC}\,v^2$$

where v is the terminal recoil velocity of the fragments and $\mu_{A,BC}$ is the reduced mass. Changing the pump wavelength changes v, and thus the time for fragments separation (bond breaking) and $\tau_{1/2}$ changes in a consistent way depending on the PES. Another effect that may shift $\tau_{1/2}$ in the opposite direction is that as E increases, the travel distance increases. This change in R_0 in general is small, because of the steep slope of the PES near R_0. From the changes in $\tau_{1/2}$ and the shape of the observed transients on- and off-resonance, one can characterize the dynamics on V_1.

Femtosecond alignment. The reaction ABC* → A + BC has been discussed so far as if its configuration space were one-dimensional (with no centrifugal contribution), the only parameter being the distance of A from the center-of-mass of BC. However, the angular part of the potential may be important. As an example, the repulsion of bending ABC would generate a torque on BC during the reaction. This time-dependent evolution of angular momentum is related to the rotational alignment and can be probed by using FTS and polarizing the femtosecond pulses. Transients taken with parallel pump and probe polarizations can be compared with those taken with perpendicular polarizations, as is done with time-integrated experiments (*31*).

The time dependence of alignment and angular momenta is reflected in two types of measurements (*32*). First, the angular part of the potential may lead to different values of $\tau_{1/2}$'s depending on the final angular momentum state of the BC fragment. Second, the loss of alignment at early times would reflect the degree of the torque that causes rotations in the BC fragment. Because the BC fragment would probably be produced in a distribution of angular momentum states and not in one state, the coherence time would be shorter than the rotational time of the fragment, as discussed in (*32*).

The femtochemistry apparatus. Two technologies are involved in much of the femtochemistry (as well as the picochemistry) studies under collisionless conditions: molecular beams and the generation and characterization of ultrashort laser pulses. The laser system built at Caltech is based on the pioneering design provided by Shank and colleagues (*27*). They have shown that 90-fs pulse widths at 100-MHz repetition rate can be obtained from a colliding-pulse mode-locked ring dye laser (a CPM laser). Since then, with the use of pulse-compression and group-velocity compensation techniques, they and other groups have generated shorter femtosecond pulses; the shortest that has been obtained by the AT&T Bell Labs group is 6 fs. These pulses are amplified (Fig. 3), and pulse broadening due to group velocity dispersion in the amplifier is eliminated by a special optical arrangement. Thus femtosecond pulses are generated at different wavelengths, opening up a number of possibilities. The characterization of the pulses is made by standard auto- and cross-correlation techniques. For subpicosecond and picosecond experiments, two synchronously pumped dye lasers (with pulse-compression capability) are used in similar arrangements.

Experiments on rotationally and vibrationally cold molecules can be performed with a molecular beam appartus (that uses a pulsed, seeded, supersonic beam) that has electron impact and laser ionization, time-of-flight mass spectrometric, and LIF capabilities. LIF is a very sensitive method (*33*) of detection, and the cooling of molecules by supersonic expansions simplifies the spectra greatly (*34*). The fragment of interest is identified with the mass spectrometer, so there is mass and quantum-state resolution. The laser beams intersect the molecular beam (or the gas) in a very small overlap zone. The time at which the initial laser pulse arrives at this zone marks the beginning of the experiment and establishes the zero-of-time; the probe pulse follows at the desired delay time.

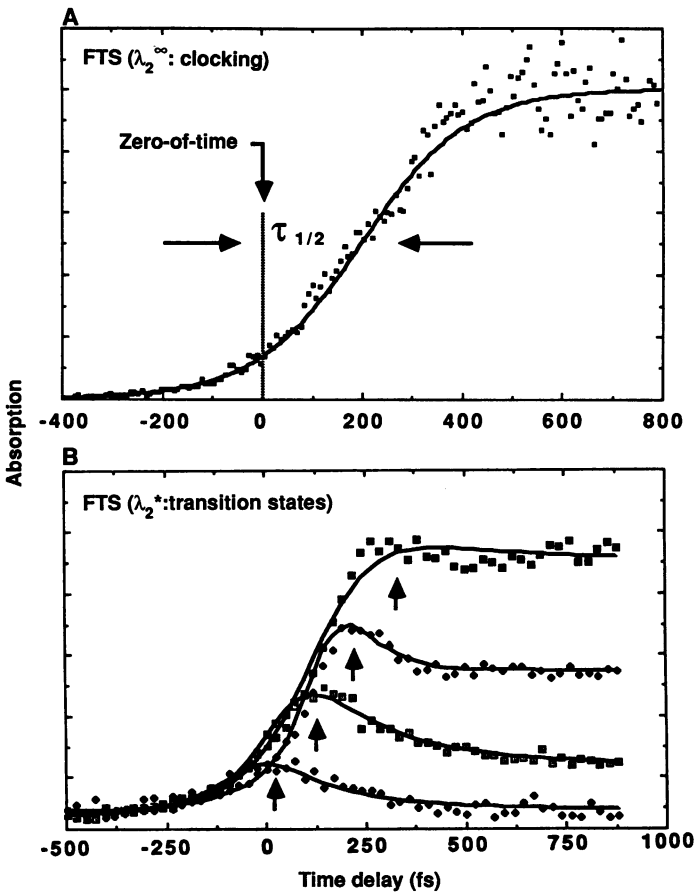

Fig. 4. FTS results for the reaction ICN*→[I···CN]‡*→I + CN. (**A**) The delayed appearance of free CN fragments (by 205 ± 30 fs) was probed at λ_2^∞ (388.5 nm). In these experiments the zero-of-time was established to determine the bond-breaking time $\tau_{1/2}$. (**B**) Transients taken for different λ_2* probings to the red wavelengths (389.7, 389.8, 390.4, and 391.4 nm) of absorption by free fragments. Note that as tuning is increased more to the red, the absorption maximum shifts to earlier times, as expected (see text).

The clocking in the experiments is determined with Michelson interferometry. By controlling the distance (optical path) between the two pulses, one determines the time (a 3-μm distance is equivalent to 10 fs), which starts when the two pulses overlap temporally at time zero. For each experiment at a chosen delay time, typically in the range of −100 to +1000 fs, the detected ionization or fluorescence signal is integrated for a sufficient length of time to yield a measure of total intensity (number density or, in some cases, product flux). The experiments are repeated at different delays and the so-called "transient" (a curve of intensity as a function of time) is constructed. The entire experiment is then repeated in the same way but at different λ_1 or λ_2. These different wavelengths are generated by non-linear methods, by using doubling and mixing crystals, or by producing a continuum of different wavelengths by focusing the femtosecond pulse on water in a jet or a cell. The Caltech apparatuses use the 40-fs pulses from the CPM laser, the 60 to 100 fs from the amplified CPM laser system, and the subpicosecond or 2 to 5 ps pulses from the synchronously pumped dye-laser systems (see Fig. 3 as an example).

Applications

Unimolecular reactions. As mentioned above, the first of these femtosecond studies dealt with unimolecular reactions. The experiments were performed on the elementary reaction:

$$ICN^* \rightarrow [I \cdots CN]^{\ddagger *} \rightarrow I + CN$$

The pump pulse was at 307 nm and the probe pulse was set at 388.5 nm (the absorption peak for free CN fragments) or detuned by as much as 10 nm to detect perturbed CN at these wavelengths through LIF. As anticipated, when tuning to the perturbed CN fragment absorption, the transients exhibit a buildup and a decay characteristic of the short-lived ($\sim 10^{-13}$ s) transition states. On-resonance absorption of the free CN fragment gives a rise delayed from $t = 0$ by $\tau_{1/2} = 205 \pm 30$ fs (see Fig. 4).

The time for bond breaking depends on the characteristics of the PES. In the simple case of a one-dimensional PES, the clocking time is directly related to the repulsion length scale (L) between the fragments (*20–22*):

$$\tau_{1/2} = L/v \ln (4E/\gamma)$$

where γ is the half-width of the probe-pulse window, and the potential is $V(R) = Ae^{-R/L}$. This formula defines the fundamentals of bond breaking: dissociation of the bond depends on the point of probing on the PES, and the time is determined by the energy of recoil ($E = \frac{1}{2} \mu v^2$) and steepness of the potential. The characteristic time $T_{1/2}$ in this case is simply the time for the potential to drop to a value equal to γ. For the ICN experiment, L was deduced to be 0.8 Å. The transition states (Figs. 4 and 5) survive for only ~50 fs or less depending on the region probed on the PES.

Theoretically, these observations were reproduced with classical-mechanical (*21, 22, 35*) as well as quantum-mechanical (*36*) treatments of the dissociation (see Fig. 5). Even kinetic equations can describe the general behavior of the transients (*21, 22*). In general, however, the PESs are more complex and the data are better inverted to obtain the shape. Such a procedure has been developed and applied to the ICN reaction (*37*).

To learn about the reaction trajectory to different final CN rotational states, $\tau_{1/2}$ was measured for different angular momentum states (*21, 22*). The femtosecond alignment was also measured. From these experiments information was obtained on the magnitude of the torque between I and CN (angular part of the PES) and on the extent to which coherence was lost among the different product states. When these experiments are completed, much should be learned about the PES and the real-time trajectories that produce the different product states. Shortening the pulses further might help resolve crossings of PESs, coherence and trapping, as discussed below.

Extension to bimolecular reactions. The above examples illustrate the potential to conduct real-time femtochemistry observations of the dynamics of a wide variety of photon-induced unimolecular reactions, both dissociations and isomerizations. But the field of chemical dynamics is broader than this and must include bimolecular reactions. Most complex reactions involve a number of elementary steps, many of which are bimolecular in nature. For such reactions, it is highly desirable to be able to observe the bimolecular collision itself in real time.

A new problem arises for bimolecular reactions that is not a concern for the unimolecular case. For a unimolecular reaction, the reaction begins when the laser pulse initiates excitation. Thus the zero-of-time is well defined, and the interval between the firing of this laser pulse and the subsequent probe laser pulse represents the actual amount of time that the reaction has been taking place. For a bimolecular reaction, whether in bulk or in crossed beams, there is no comparable way to establish the zero-of-time: Reagent molecules first must find each other (on a time scale of nanoseconds to microseconds) and then collide before reaction could possibly occur. The long nanosecond to microsecond times between collisions

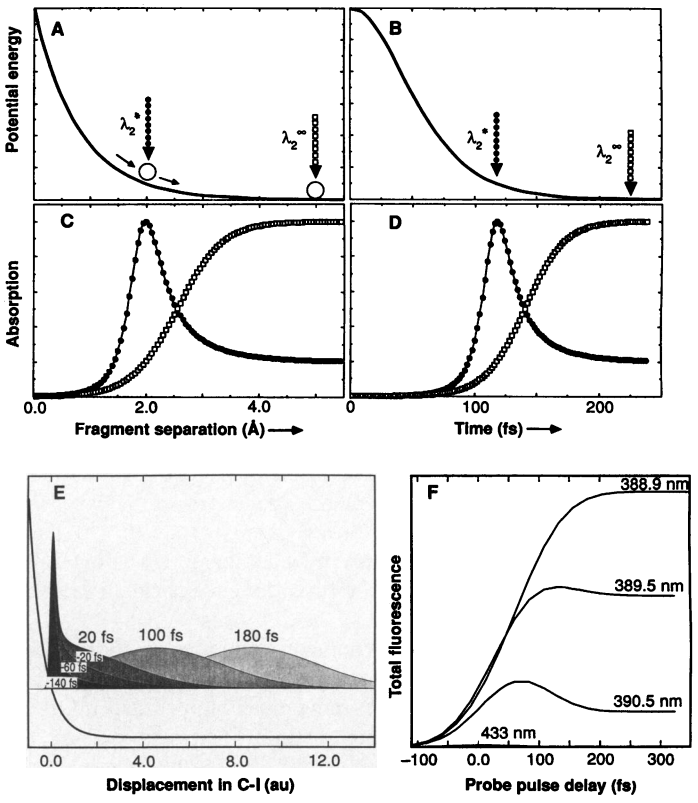

Fig. 5. (**A** through **D**) Theoretical classical-mechanics calculations for the reaction $ICN^* \rightarrow [I \cdots CN]^{\ddagger *} \rightarrow I + CN$. The potential energy as a function of (A) fragment separation [$V(R)$] and (B) time [$V(t)$]. By 200 fs, the bond is essentially broken. The probing at λ_2^* and λ_2^∞ is depicted on the PES, and the calculated FTS signals are shown at these two wavelengths of probing as a function of (C) fragment separation [$A(R)$] and (D) time [$A(t)$] ($\gamma = 250$ cm^{-1}, and $L = 0.8$ Å). This simple theory reproduces the major features of the experiments (see text). (**E** and **F**) Theoretical quantum mechanical calculations for the same reaction. (E) The wave packet propagation with time, executing ~5 Å in 200 fs. (F) The expected FTS signal is shown and again reproduces the experimental observations [see (*36*)].

represent an uncertainty as to when the reactants collided with one another. Thus determining the time of formation and decay of transient collision complexes with lifetimes of only femtoseconds to picoseconds would seem hopeless.

However, a special method enables one to establish the zero-of-time within an uncertainty governed by the laser pulse duration only. The dynamics of a whole class of bimolecular reactions can now be studied in real time. The first of these experiments, by Scherer *et al.* (*38*) in collaboration with R. B. Bernstein, has been conducted in the picosecond, rather than femtosecond, time domain, but the principle is the same. The method involves the use of a beam of a van der Waals "precursor molecule" containing the potential reagents in close proximity. Weak molecular complexes were used, as pioneered by Wittig's and Soep's groups in studies of product-state distribution (*39*), so the zero-of-time can be established and hence the course of the reaction can be followed in real time. For the reaction studied (*38*),

$$H + OCO \rightarrow [HOCO]^{\ddagger} \rightarrow OH + CO$$

the precursor molecule was IH $\cdots$ OCO, which was formed in a free-jet expansion of a mixture of HI and CO_2 in an excess of helium carrier gas. Such van der Waals complexes have a favorable geometry that limits the range of impact parameters and angles of attack of the H on the OCO (*39*).

To clock the reaction, an ultrashort laser pulse initiates the experiment by photodissociating the HI, ejecting a translationally hot H atom in the general direction of the nearest-neighbor O atom in the CO_2 (Fig. 6). A probe laser pulse tuned to a wavelength suitable for detection of the OH was delayed relative to the photolysis pulse with Michelson interferometry. The OH appeared after a delay of a few picoseconds from the initiation pulse. This experiment directly measures the lifetime of the $[HOCO]^{\ddagger}$ collision complex at the available energy of the collision and confirms that the reaction is not direct mode in nature (*40*). The lifetime depends on the translational energy, and is shorter at high collision energies. A new series of femtosecond-pulse experiments is being undertaken in order to follow the formation and decay of the collision complex in the femtosecond region and to study the effect of limited impact parameter, an important feature of this approach, on the reaction dynamics. Comparison with classical trajectory calculations, based upon the ab initio calculated PES is also important (*41*).

This technique promises to be applicable to a wide variety of bimolecular reactions, including not only those involving long-lived collision complexes that last for picoseconds, but also direct-mode reactions with transition-state lifetimes in the femtosecond range. Transition-state detection, as described for the half-collision case, should allow for new measurements in the transition region of the

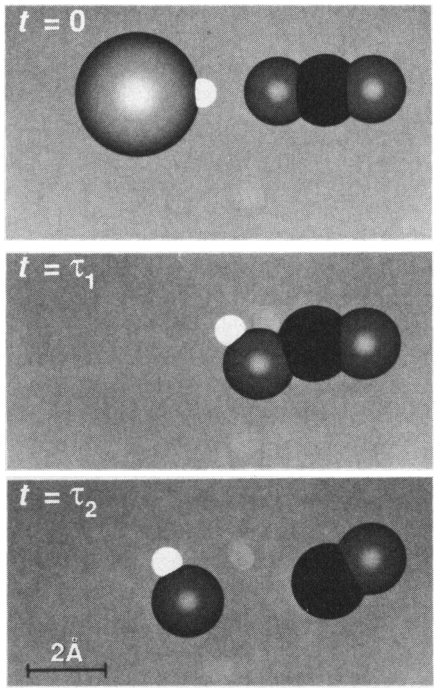

Fig. 6. Snapshots schematic representation of the bimolecular reaction H + CO_2→ $[HOCO]^{\ddagger}$ →HO + CO. A precursor geometry of IH $\cdots$ CO_2 is used. The clocking pulse, which sets the zero-of-time, breaks the HI bond and produces H atoms to react with CO_2. The probe pulse monitors the produced OH fragments as a function of the delay time between pump and probe pulses. In this way the collision complex $[HOCO]^{\ddagger}$ of the reaction can be studied in real time (see text).

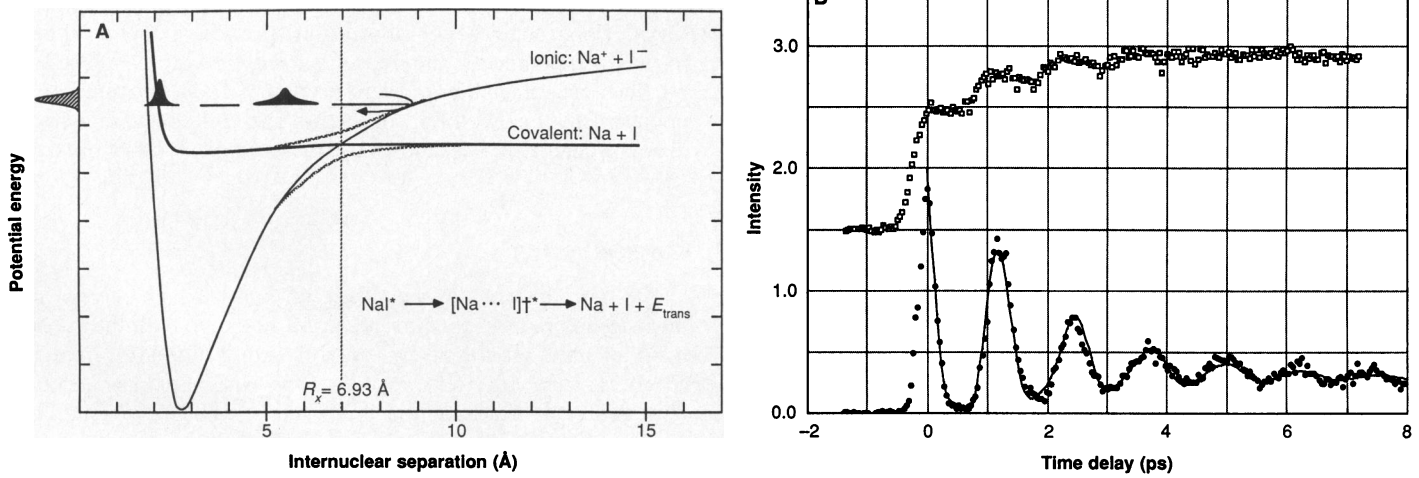

Fig. 7. (**A**) Potential energy curves for reactions of alkali halides displaying the ionic and covalent states of the reaction. The pump pulse (λ_1), indicated by the bell-shaped curve on the vertical axis, takes the salt Na^+I^- to the covalent surface NaI*. As the bond stretches $[Na \cdots I]^{\ddagger}$*, the probe (λ_2) monitors the evolution of the wave packet (indicated by the bell-shaped curve moving along R) of dissociating molecules in the transition region (λ_2*) and at "infinite" separation ($\lambda_2\infty$). Note the avoided crossing between the ionic and covalent curves and the possible trapping of the packet that may result from this electron harpooning at the crossing point, R_x (see text). (**B**) FTS experimental results for the reaction of alkali halides NaI*→ $[Na \cdots I]^{\ddagger}$*→Na + I. The transient at the bottom shows the oscillatory (resonance) behavior of the wave packet as it moves back and forth between the covalent and ionic curves of (A). Each time the packet comes near the crossing point there is a probability of escape (~0.1), which is observed as a damping of the oscillations. The resonance frequency gives the round trip time in the well. The experiment was performed by exciting at 310 nm and detecting off-resonance to the transition of free Na atom at 589 nm. When detecting on-resonance, the transient at the top was obtained. On-resonance, the trajectory is "integrated" over the entire distance and one expects an integration of the oscillation to yield plateaus, with steps given exactly by the resonance frequency, as observed experimentally. This result is a clear demonstration of the idea of FTS (see text).

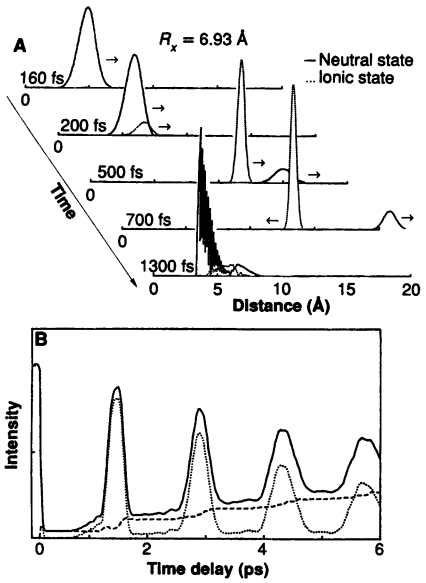

Fig. 8. Theoretical quantum-mechanical calculations of the reaction of NaI. (**A**) Snapshots of the wave packet as it propagates from the initial covalent configuration, before and after the crossing point (see Fig. 7A). Note the "splitting" of the packet to neutral (solid line) and ionic (dotted line) states as a function of time. These are typical results for the different λ_1s studied. (**B**) The expected FTS transient (at λ_1 = 300 nm) when detecting free fragment [($\lambda_2\infty$), steps with plateaus] and in the transition region [(λ_2*), oscillatory behavior]. The solid line is the total signal. The calculations are consistent with experiments and with the derived parameters obtained by the experiments. The calculations are given in (*44*) by Engel *et al.*

full collision with the zero-of-time being known accurately with femtosecond time resolution. The dynamics for this class of bimolecular reactions with known precursor geometry may be different from those averaged over all impact parameters and orientations, and studies of femtosecond alignment should provide an additional dimension for probing such effects and differences (*32*).

Reactions from the "alkali age": Covalent-to-ionic crossings. The process of direct bond breaking discussed thus far occurs on dissociative PESs, and molecules are in "transition" for only ~50 fs, as evidenced by the rise and decay observed in the ICN experiments and confirmed by theory. If, however, in the process of falling apart, the system encounters a well in the PES, or if there is more than one degree of freedom involved, trapping can occur. As a result, the system may exhibit characteristics indicative of quasibound states, or resonances. In real time, manifestation of these trapping resonances would be a slowdown in the appearance of free fragments and possibly the appearance of oscillations reflecting the vibrational resonance frequency of the wave packet of the dissociating fragments.

The classic reactions of alkali metal–halogen are prototype systems for such studies. This class of reactions was studied in the "alkali age" (*1*) of molecular-beam scattering of alkali metal (M) and halogen (X). Observing their real-time behavior is of great interest to current studies in the "femto age." Because of the difference in the ionization potential of M and the electron affinity of X, the energy of $M^+ + X^-$ is greater than that of M + X. In the ground state, the molecule is ionic (M^+X^-), and this state correlates with the $M^+ + X^-$ (see Fig. 7A). Hence, the covalent potential curve (M + X) crosses the ionic (Coulombic) curve. Because of this crossing (or avoided crossing) at certain M···X separation (R_x), electron "harpooning" occurs, that is, the electron is transferred at a relatively large R_x. The PESs for such important processes have been described in a classic series of papers by Berry [for a review of theoretical and chemical studies, see (*42*)].

In the femtochemistry experiments (*18, 19*), the initial pulse at λ_1 takes the molecule from the M^+X^- ground state to the covalent surface MX*. The second pulse probes the reaction at λ_2* (transition-state region) and at $\lambda_2\infty$ (final product; in this case Na):

$$MX^* \rightarrow [M\cdots X]^{\ddagger *} \rightarrow M + X \qquad (M = Na;\ X = I,\ Br)$$

En route to products, the $[M\cdots X]^{\ddagger *}$ transition-state molecules "decide" between ionic and covalent paths: Either the packet of MX* is trapped on the adiabatic potential curve or it dissociates by following the diabatic curve. The two cases have entirely different temporal behavior and, if there is trapping, the frequency and amplitude of the oscillations provides details of the nature of the surfaces and the strength of the coupling. Comparison with theory (*43*) can then be made.

The experiments show (Fig. 7B) a striking oscillatory behavior (when probing at λ_2*) that persists for many picoseconds (~10 oscillations) in the case of NaI, and for less than a few picoseconds (~2 oscillations) for the NaBr case. Probing on-resonance (at $\lambda_2\infty$) gives a rise with plateaus separated by the same oscillations frequency. This on-resonance "integration" of the trajectories is a clear demonstration of the concept of FTS discussed earlier.

The average period for the NaI reaction is 1.25 ps, which corresponds to a frequency of 27 cm^{-1}. The packet for NaI is effectively trapped in the adiabatic well en route to products, and the observed oscillations represent "pulses of Na atoms" leaving the well. Since the oscillation damping time for NaI is ~10 ps, one crossing on the outward phase per oscillation (~1 ps) has a probability of about 0.1 to escape from the well. For NaBr, the frequency of oscillation is similar in magnitude, but severe damping is observed. Thus the crossing for NaBr is much more facile than for NaI, consistent with theoretical expectation. In (*18*) and (*19*) theory was compared with experiments and obtained the Landau-Zener probability of escape, the anharmonicity of the PES, and the coupling between the covalent and ionic curves. An interesting question is how the "dephasing" and spread of the wave packet influences the dissociation rate, as determined by the decay of the oscillations. The experiments do show manifestations of this decay and spreading, and theoretical modeling of the wave packet dynamics in these prototye systems is important. Very recently these experimental results were reproduced by quantum-mechanical (*44*) and semiclassical (*45*) calculations (Fig. 8).

Real-time observations of the dynamics at different recoil energies and probing wavelengths now allow one to view the motion of the wave packet under different conditions from the Franck-Condon excitation region all the way to "infinite separation," or fragmentation, making contact with absorption spectroscopy, crossed-beam scattering experiments, and photofragment translational spectroscopy. Such experiments promise to provide rich information bearing upon the shape of the PES, curve crossings, and interactions among different degrees of freedom (resonances) in many other reactions.

Perspectives

The introduction of the "flash of light" to chemistry, with microsecond resolution, came about 40 years ago with the development of flash photolysis by Norrish and Porter (*46*). With the advances made with lasers, the time resolution continually improved over the years, reaching the "picosecond era." As a result, new studies of relaxation processes, energy transfer, and reactions in solutions emerged (*47*).

Prior to femtochemistry, molecular beams and picosecond lasers were combined, which led to studies of collision-free energy redistribution in molecules and state-to-state rates of reactions (*48*), but the time resolution was still not sufficient to directly view the process of bond breaking or bond formation. However, in femtochemistry, the "shutter speed" has reached the 10^{-15}-s regime, so it is now possible to observe chemistry as it happens—the transition-state region between reagents and products. The present limit of ~6-fs time resolution (see text) corresponds to a spatial window of ~0.06 Å

through which the atomic or fragment displacement and the PES of the reaction can be viewed.

The results given here for elementary reactions are just the beginning and more applications of this experimental approach should now be possible. This real time probing of reactions should allow for more insights into the theoretical foundation of chemical reactivity. The ultimate goal is to construct the PES and obtain the dynamics of the reaction. Although the focus in this article was on reactions under collisionless conditions, there are many analogous primary processes involving electron motion and transfer in condensed media and conformational changes in biological systems that occur on the femtosecond time scale. Femtochemical studies of reactions in condensed phases and on surfaces are natural extensions for deducing characteristics of the PES.

It appears that the future is exciting, as it is now possible to view the fundamental processes of chemical bond breaking or formation and to study the dynamics of the region of the ephemeral transition states. The strobing of these ultrafast molecular motions, stemming from this happy marriage between ultrafast lasers and chemistry, is what forms the central theme in real time femtochemistry.

REFERENCES AND NOTES

1. D. R. Herschbach, *Le Prix Nobel, 1986* (Elsevier, Amsterdam, 1987).
2. Y. T. Lee, *Science* **236**, 793 (1987).
3. J. C. Polanyi, *ibid.*, p. 680.
4. R. D. Levine and R. B. Bernstein, *Molecular Reaction Dynamics and Chemical Reactivity* (Oxford Univ. Press, New York, 1987), and references therein.
5. I. W. M. Smith, *Nature* **328**, 760 (1987).
6. R. N. Zare and R. B. Bernstein, *Phys. Today* **33**, 43 (November 1980).
7. H.-J. Foth, J. C. Polanyi, H. H. Telle, *J. Phys. Chem.* **86**, 5027 (1982).
8. D. Imre, J. L. Kinsey, A. Sinha, J. Krenos, *ibid.* **88**, 3956 (1984).
9. P. R. Brooks, R. F. Curl, T. C. Maguire, *Ber. Bunsenges. Phys. Chem.* **86**, 401 (1982); P. R. Brooks, *Chem. Rev.* **88**, 407 (1988).
10. R. B. Metz, T. Kitsopoulos, A. Weaver, D. Neumark, *J. Chem. Phys.* **88**, 1463 (1988); see also (*11*).
11. A. Benz and H. Morgner, *Mol. Phys.* **57**, 319 (1986).
12. J.-C. Nieh and J. J. Valentini, *Phys. Rev. Lett.* **60**, 519 (1988).
13. P. D. Kleiber, A. M. Lyyra, K. M. Sando, S. P. Heneghan, W. C. Stwalley, *ibid.* **54**, 2003 (1985).
14. L. R. Khundkar, J. L. Knee, A. H. Zewail, *J. Chem. Phys.* **87**, 77 (1987); N. F. Scherer and A. H. Zewail, *ibid.* **87**, 97 (1987); J. L. Knee, L. R. Khundkar, A. H. Zewail, *ibid.* **87**, 115 (1987); for a recent review, see J. L. Knee and A. H. Zewail, *Spectroscopy* **3**, 44 (1988), and references therein.
15. The name "femtochemistry" first emerged in a champagne meeting in Santa Monica, California. It was the result of R. B. Bernstein's bubbly enthusiasm for the new studies in this field. Elsewhere, the author and R. B. Bernstein have reviewed the development of reaction dynamics studies over the past 30 years, including femtochemistry.
16. N. F. Scherer, J. L. Knee, D. D. Smith, A. H. Zewail, *J. Phys. Chem.* **89**, 5141 (1985).
17. M. Dantus, M. J. Rosker, A. H. Zewail, *J. Chem. Phys.* **87**, 2395 (1987).
18. T. S. Rose, M. J. Rosker, A. H. Zewail, *ibid.* **88**, 6672 (1988).
19. M. J. Rosker, T. S. Rose, A. H. Zewail, *Chem. Phys. Lett.* **146**, 175 (1988).
20. M. J. Rosker, M. Dantus, A. H. Zewail, *Science* **241**, 1200 (1988).
21. ———, *J. Chem. Phys.* **89**, 6113 (1988).
22. M. Dantus, M. J. Rosker, A. H. Zewail, *ibid.*, p. 6128.
23. M. G. Evans and M. Polanyi, *Trans. Faraday Soc.* **31**, 875 (1935); H. Eyring, *J. Chem. Phys.* **3**, 107 (1935).
24. J. O. Hirschfelder, H. Eyring, B. Topley, *J. Chem. Phys.* **4**, 170 (1936).
25. M. Karplus, R. N. Porter, R. D. Sharma, *ibid.* **43**, 3258 (1965); see also (*26*).
26. K. J. Laidler, *Theories of Chemical Reaction Rates* (McGraw-Hill, New York, 1969), and references therein.
27. C. V. Shank, *Science* **233**, 1276 (1986), and references therein.
28. See A. Gallagher, in *Physics of Electronic and Atomic Collisions*, S. Datz, Ed. (North-Holland, Amsterdam, 1982), p. 403.
29. B. A. Collings, J. C. Polanyi, M. A. Smith, A. Stolow, A. W. Tarr, *Phys. Rev. Lett.* **59**, 2551 (1987).
30. E. J. Heller, *Acc. Chem. Res.* **14**, 368 (1981).
31. See, for example, the special issue on dynamical stereochemistry, *J. Phys. Chem.* **91**, 5365–5509 (1987).
32. A. H. Zewail, *Faraday Discuss. Chem. Soc.*, in press.
33. R. N. Zare and P. J. Dagdigian, *Science* **185**, 739 (1974).
34. R. E. Smalley, L. Wharton, D. H. Levy, *Acc. Chem. Res.* **10**, 139 (1977).
35. R. Bersohn and A. H. Zewail, *Ber. Bunsenges Phys. Chem.* **92**, 373 (1988).
36. S. O. Williams and D. G. Imre, *J. Phys. Chem.*, in press.
37. R. B. Bernstein and A. H. Zewail, *J. Chem. Phys.*, in press.
38. N. F. Scherer, L. R. Khundkar, R. B. Bernstein, A. H. Zewail, *ibid.* **87**, 1451 (1987); N. F. Scherer, C. Sipes, R. B. Bernstein, A. H. Zewail, unpublished results.
39. G. Radhakrishnan, S. Buelow, C. Wittig, *J. Chem. Phys.* **84**, 727 (1986), and references therein; C. Jouvet and B. Soep, *ibid.* **80**, 2229 (1984).
40. J. Brunning, D. W. Derbyshire, I. W. M. Smith, M. D. Williams, *J. Chem. Soc. Faraday Trans.* II, **84**, 105 (1988); C. W. Larsen, P. H. Stewart, D. Golden, *Int. J. Chem. Kinetics.* **20**, 27 (1988), and references therein.
41. G. Schatz, M. S. Fitzcharles, L. B. Harding, *Faraday Discuss. Chem. Soc.* **84**, 359 (1987).
42. R. S. Berry, in *Alkali Halide Vapors*, P. Davidovits and D. L. McFadden, Eds. (Academic Press, New York, 1979), and references therein.
43. R. Grice and D. R. Herschbach, *Mol. Phys.* **27**, 159 (1974); S. A. Adelman and D. R. Herschbach, *ibid.* **33**, 793 (1977).
44. V. Engel, H. Metiu, R. Almeida, R. A. Marcus, A. H. Zewail, *Chem. Phys. Lett.* **152**, 1 (1988); S. E. Choi and J. C. Light, *J. Chem. Phys.*, in press.
45. R. A. Marcus, *Chem. Phys. Lett.* **152**, 8 (1988).
46. R. G. W. Norrish and G. Porter, *Nature* **164**, 658 (1949); *Discuss. Faraday Soc.* **17**, 40 (1954).
47. For reviews of the early and leading contributions by the research groups of P. M. Rentzepis, K. B. Eisenthal, R. M. Hochstrasser, W. Kaiser, E. Ippen, C. Shank, R. Alfano, S. Shapiro, M. Windsor, G. Porter, G. W. Robinson, and others, see: P. M. Rentzepis and K. J. Kaufman, *Acc. Chem. Res.* **8**, 408 (1975); K. B. Eisenthal, *ibid.*, p. 118; R. M. Hochstrasser and R. B. Weisman, in *Radiationless Transitions*, S. H. Lin, Ed. (Academic Press, New York, 1980), p. 317; A. Laubereau and W. Kaiser, *Rev. Mod. Phys.* **50**, 607 (1978); S. L. Shapiro, Ed., *Ultrashort Light Pulses*, vol. 18 of *Topics in Applied Physics* (Springer-Verlag, New York, 1977); C. V. Shank, E. P. Ippen. S. L. Shapiro, Eds., *Chemical Physics 4* (Springer-Verlag, New York, 1978).
48. For recent reviews, see P. M. Felker and A. H. Zewail, *Adv. Chem. Phys.* **70**, 265 (1988), and references therein; A. H. Zewail, *Faraday Discuss. Chem. Soc.***75**, 315 (1983); and (*14*).

49. Supported by the Air Force Office of Scientific Research and by the National Science Foundation. I thank the members of my group, past and present, whose talents, dedication and excitement have made this undertaking possible and enjoyable. The collaborations with my colleagues R. Marcus (on unimolecular reactions), R. Bernstein (on bimolecular reactions), and R. Bersohn (on half-collision processes) have enriched the excitement about this research and added important contributions. I thank M. Dantus, M. Rosker, T. Rose, C. Sipes, and H. Levy for their help in the preparation of the manuscript, and the Guggenheim Foundation for making it possible to finalize it while in France. Prior to publication, the manuscript was read by many colleagues and I am grateful for their efforts and advice. Contribution No. 7836 of the Arthur Amos Noyes Laboratory.